Supporting Information

Autologous Cancer Cryoablation Mediated Nanovaccine Augments Systematic Immunotherapy

Zhongyang Yu[1,2,#], Dawei Wang[3,4,#], Yuxia Qi[1,2], Jing Liu[3,4], Tian Zhou[2,], Wei Rao[3,4,*], and Kaiwen Hu[2,*]*

[1]Beijing University of Chinese Medicine, Beijing, 100029, China. [2]Oncology Department, Dongfang Hospital, Beijing University of Chinese Medicine, Beijing, 100078, China. [3]Technical Institute of Physics and Chemistry, Chinese Academy of Sciences, Beijing 100190, China. [4]School of Future Technology, University of Chinese Academy of Sciences, Beijing 100049, China.

E-mail: H.K.:kaiwenh@163.com, W.R.: weirao@mail.ipc.ac.cn , T.Z.: tzhou@bucm.edu.cn

Abbreviations: N-(methoxycarbonyl) maleimide: N-M-Mal, Pluronic F127: PF-127, Pluronic F127–chitosan nanoparticles (NPs), N-(methoxycarbonyl) maleimide (Mal)-cross-linked Pluronic F127–chitosan nanoparticles (MNPs), astragalus polysaccharide: APS, APS-encapsulated MNPs: AMNPs.

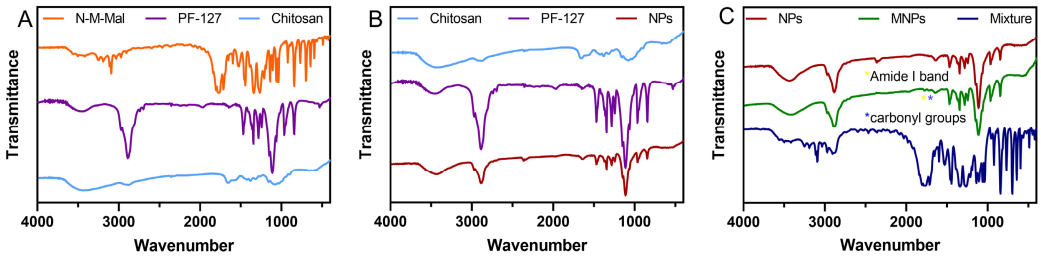

Figure S1. Typical FTIR spectra of N-M-Mal, PF-127, chitosan, NPs, MNPs, and a simple mixture of NPs with N-M-Mal. (A) Typical FTIR spectra of basic raw materials, N-M-Mal, PF-127, and chitosan. (B) The crosslink formation of NPs was confirmed by the characteristic bands of PF-127 and chitosan. (C) The conjugation of NPs with N-M-Mal was qualitatively confirmed by the appearance of some new bands.

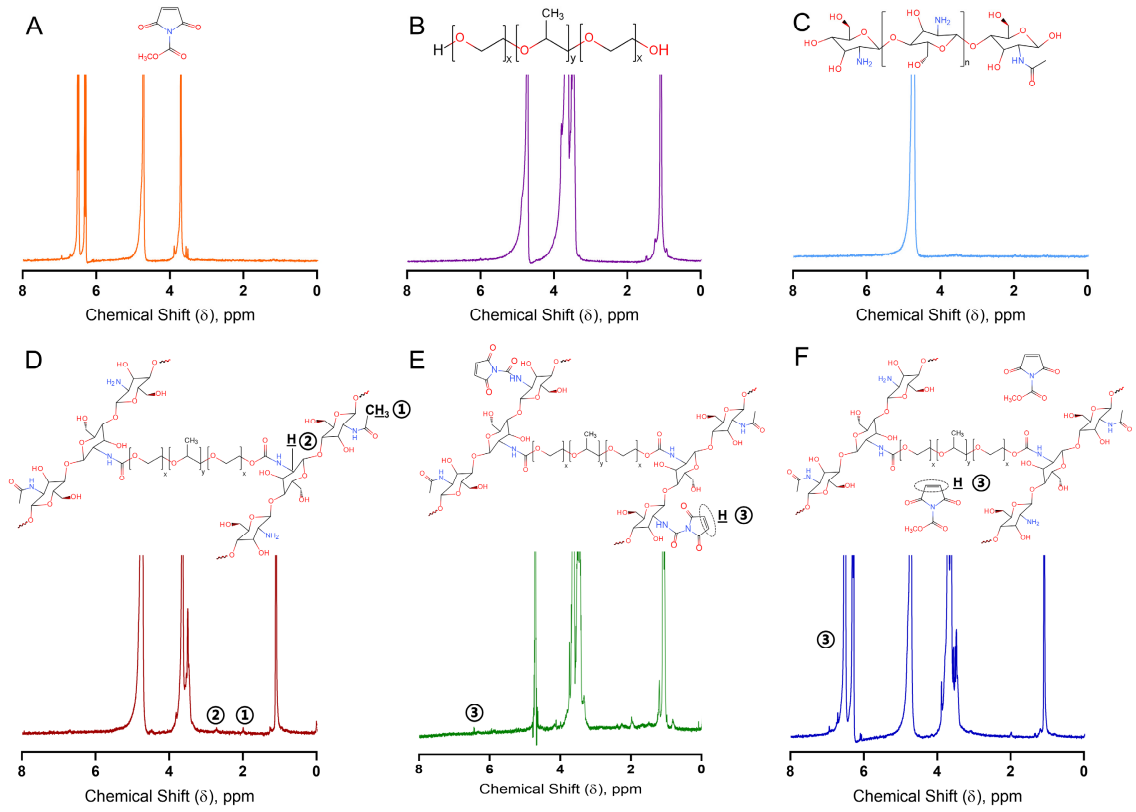

Figure S2. Typical 1H NMR spectra of the different species show the successful crosslink formation of MNPs. (A) N-M-Mal. (B) PF-127. (C) Chitosan. (D) NPs. (E) MNPs. (F) Simple mixture of N-M-Mal and NPs.

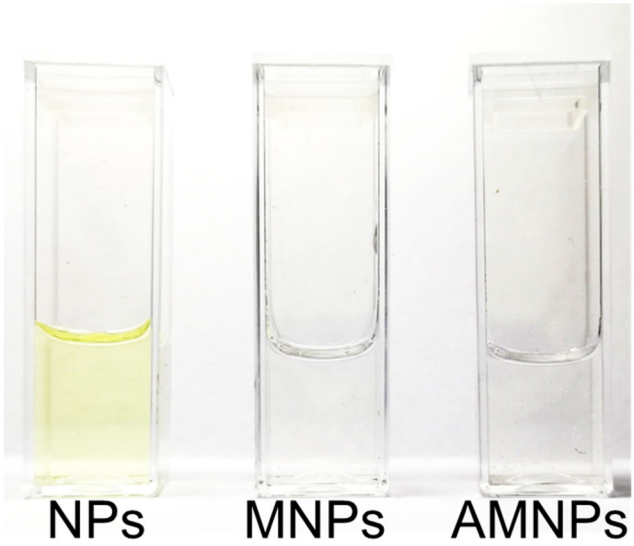

Figure S3. Optical image of NPs, MNPs and AMNPs dispersed in phosphate buffer solution (PBS) (pH = 7.4).

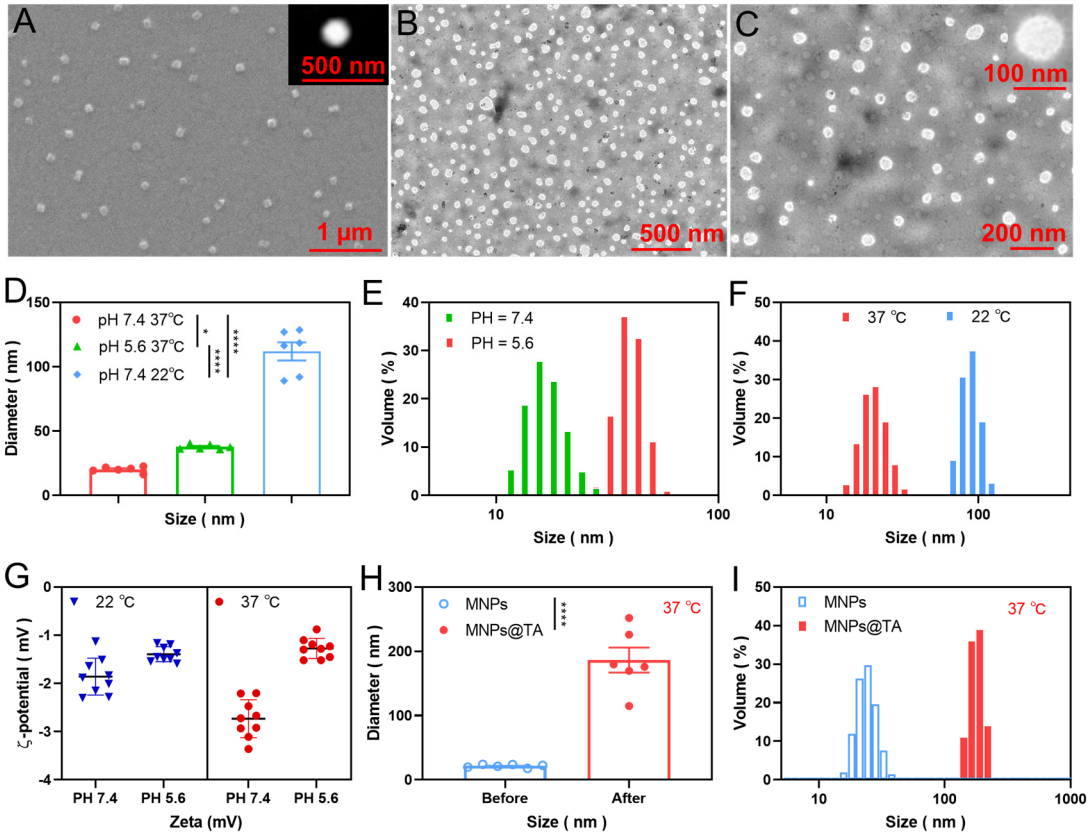

Figure S4. Characterization of N-(methoxycarbonyl) maleimide (Mal)-cross-linked Pluronic F127–chitosan nanoparticle (MNPs). (A) A typical SEM image of MNPs at room temperature. (B) and (C) The typical TEM images of MNPs at room temperature (about 22°C). (D) Size of MNPs at different pH values and temperatures in PBS solution(F), and typical dynamic light scattering (DLS) data (E, 37 °C; F, pH = 7.4). (G) Zeta potential of MNPs at different pH values and temperatures in PBS solution. (H) Size and typical DLS data (I) of MNPs before and after antigen-capture at different temperatures in PBS solution (pH = 7.4, 37 °C). *p < 0.05, **p < 0.01, ***p < 0.001, ****p < 0.0001.

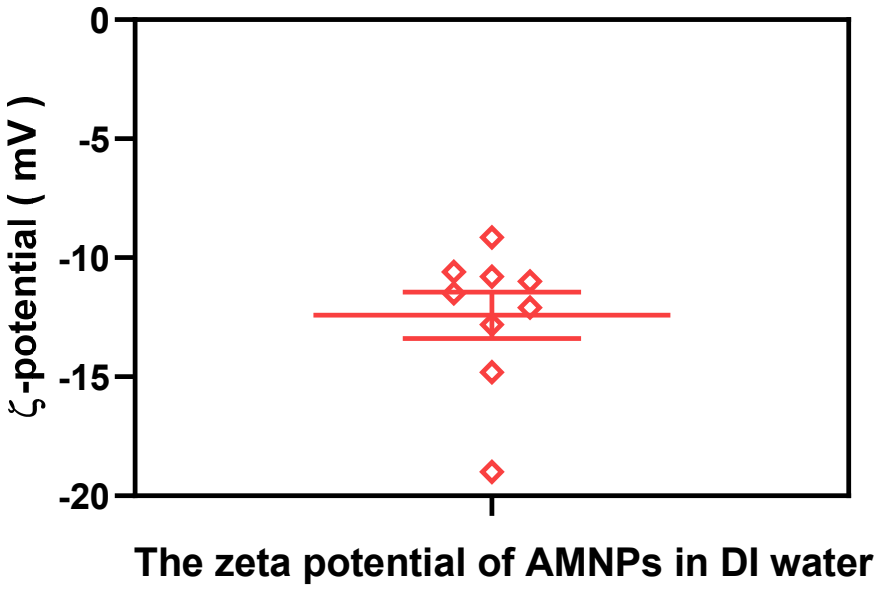

Figure S5. The zeta potential shows that the AMNPs have a negatively charged surface (-12.42 ± 0.98 mV, in DI water).

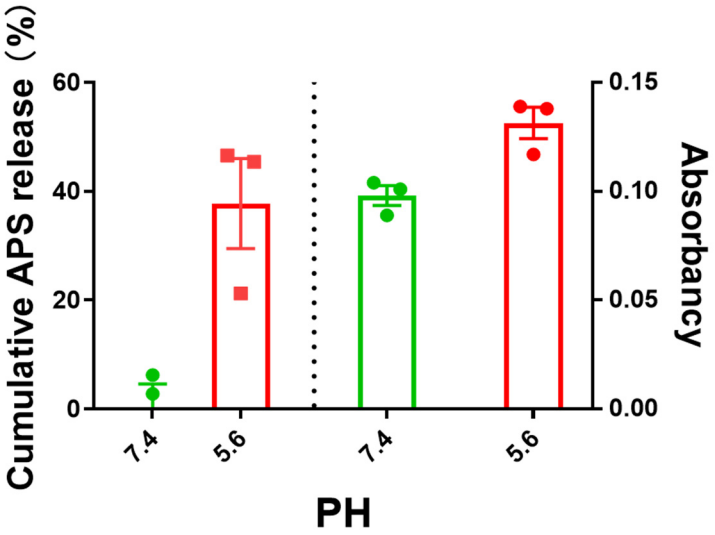

Figure S6. The APS release behaviors of pH responsive AMNPs and the absorbance after Phenol-sulfuric acid method.

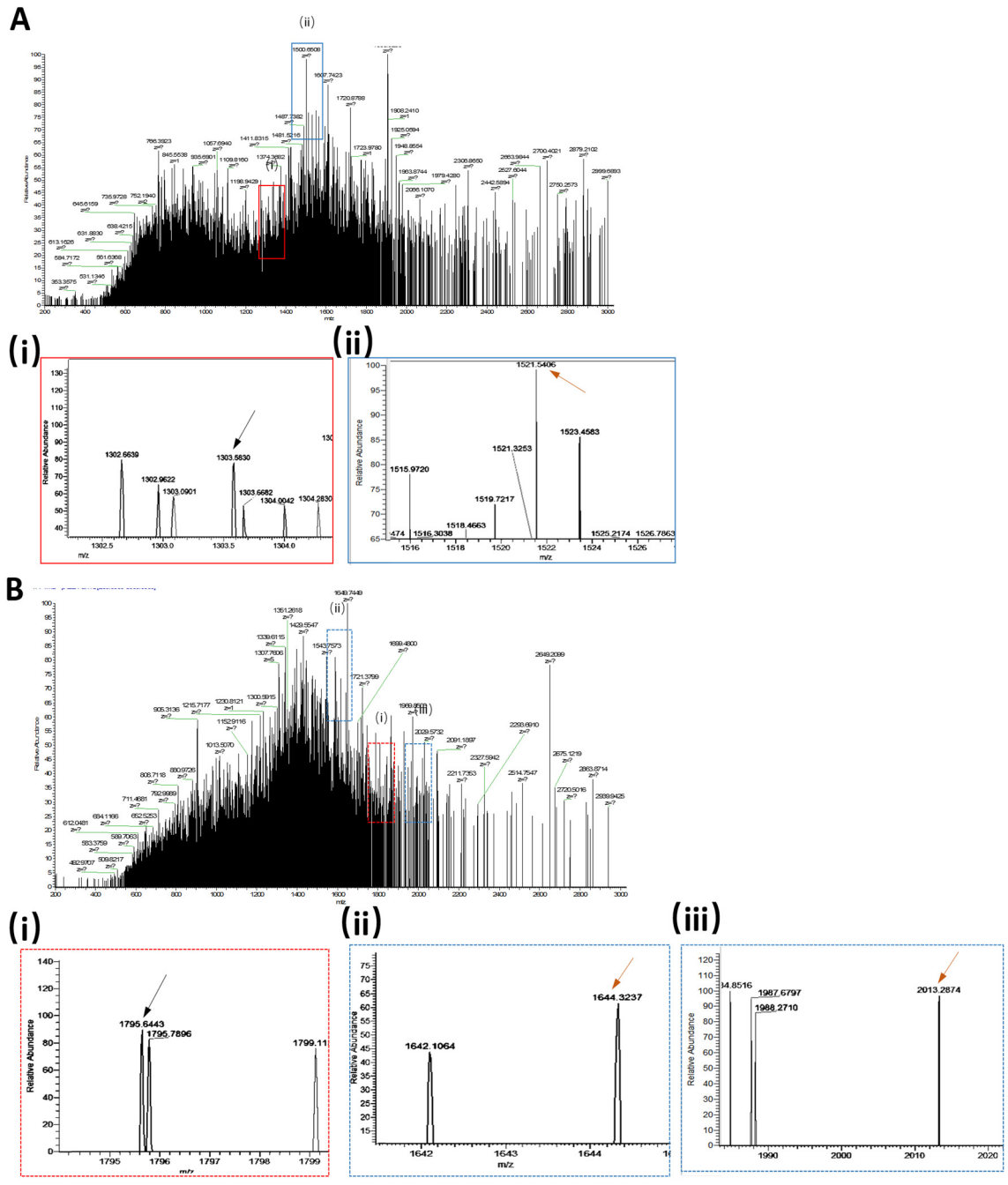

Figure S7. Typical mass spectrum of NPs, MNPs, APS and AMNPs. (A) NPs. (i) Spectrum distribution of NPs around 1303. (ii) Spectrum distribution of NPs around 1521. (B) MNPs. (i) Spectrum distribution of MNPs around 1795. (ii) Spectrum distribution of MNPs around 1644. (iii) Spectrum distribution of MNPs around 2013.

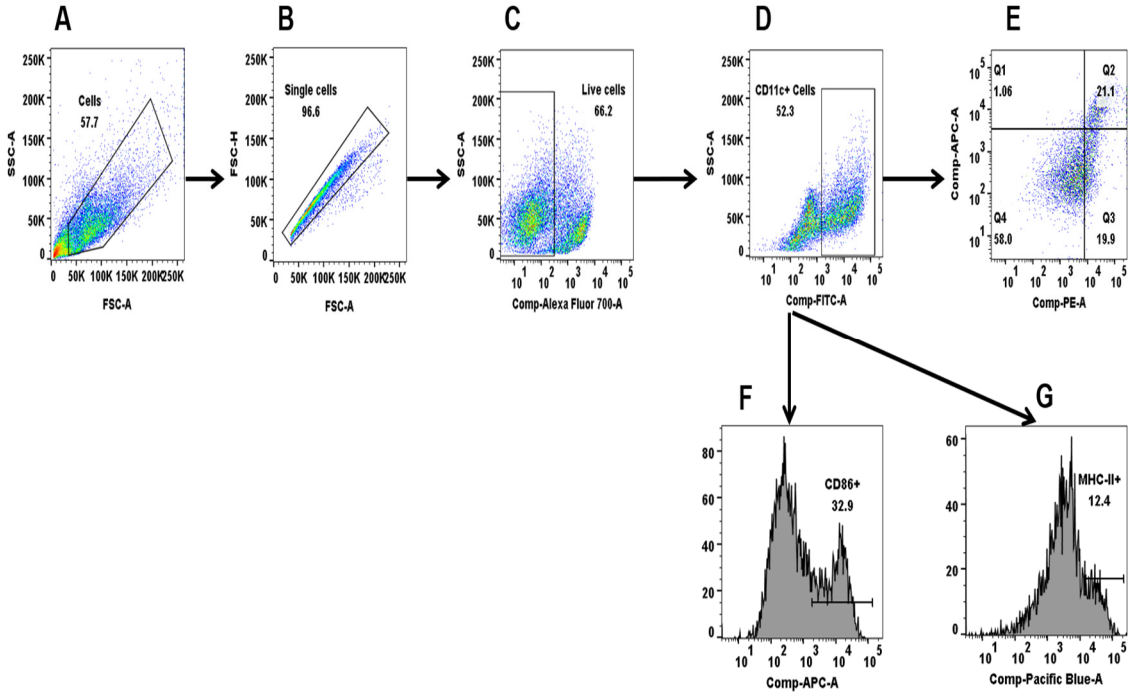

Figure S8. Gating strategy used for *in vitro* flow cytometry experiments. (A) All events were plotted side scatter vs. forward scatter, and debris was gated out. Next (B) single cells and (C) live cells were selected. Then, CD11c+ cells were selected for DCs (D). Next, CD11c+ cells were quantified for CD40+(F), CD86, or MHC-II positivity (E).

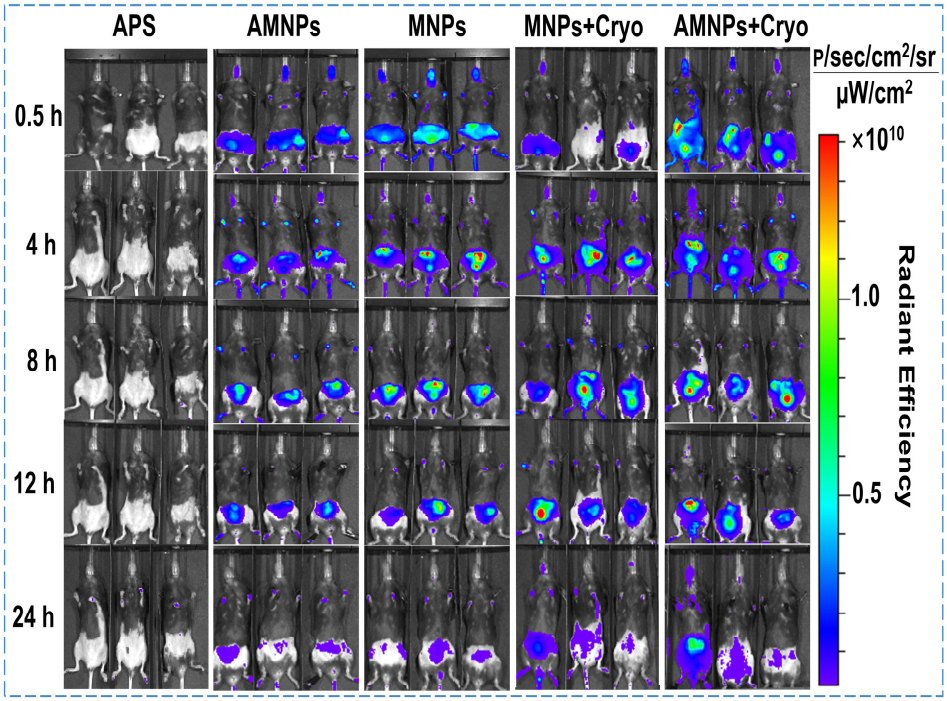

Figure S9. Intravital imaging of mouse abdomen. APNPs and MNPs w/wo cryosurgery are enriched in the inguinal lymph nodes on both sides of the mouse and are metabolized by the kidney-bladder.

Figure S10. Representative photographs on Day 30. From left to right: saline group, APS group, MNPs group, AMNPs group, Cryoablation group, APS+Cryo group, MNPs+Cryo group, AMNPs +Cryo group.

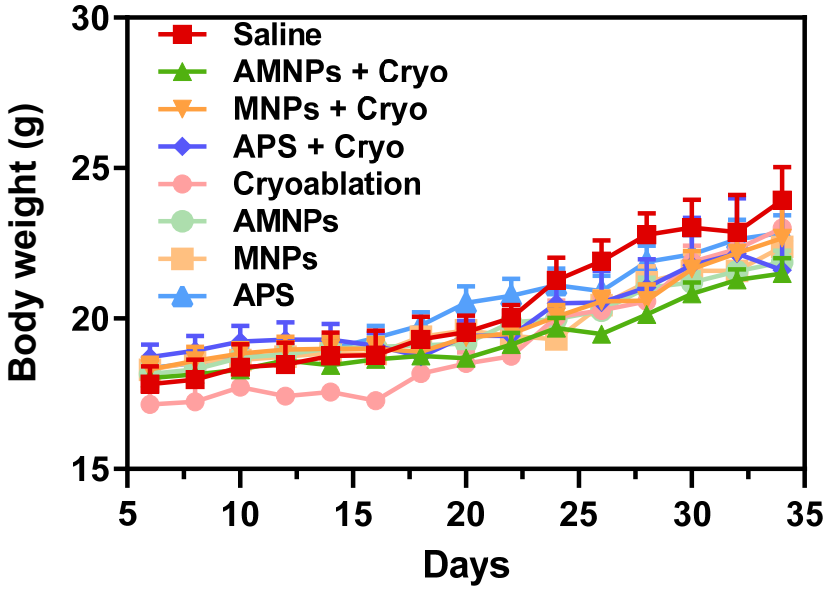

Figure S11. Bodyweight curve after various treatments

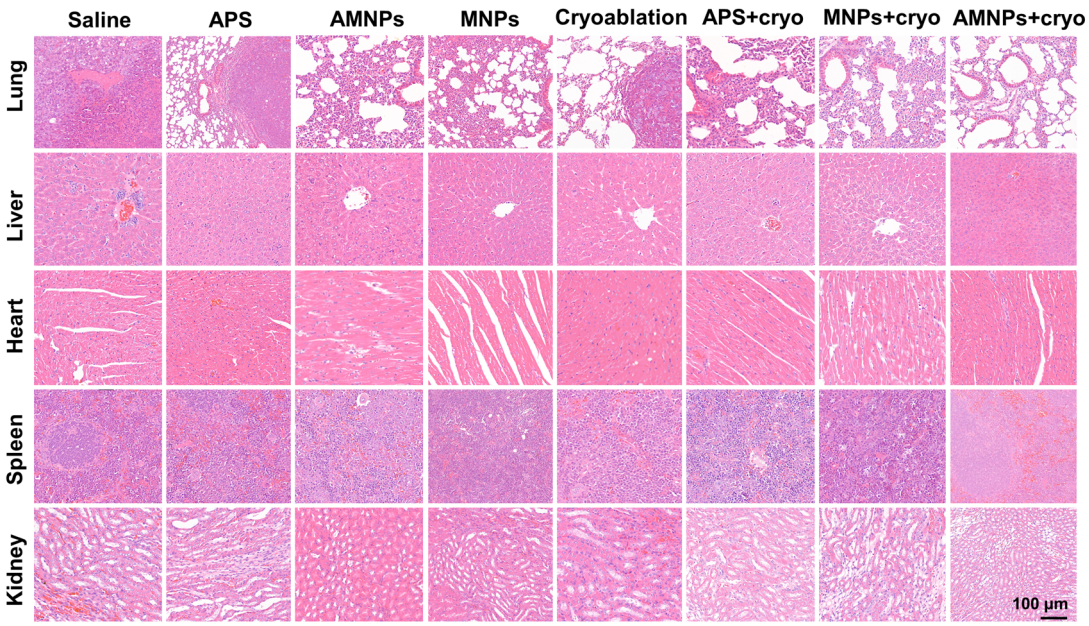

Figure S12. H&E staining images for distant tumors after various treatments.

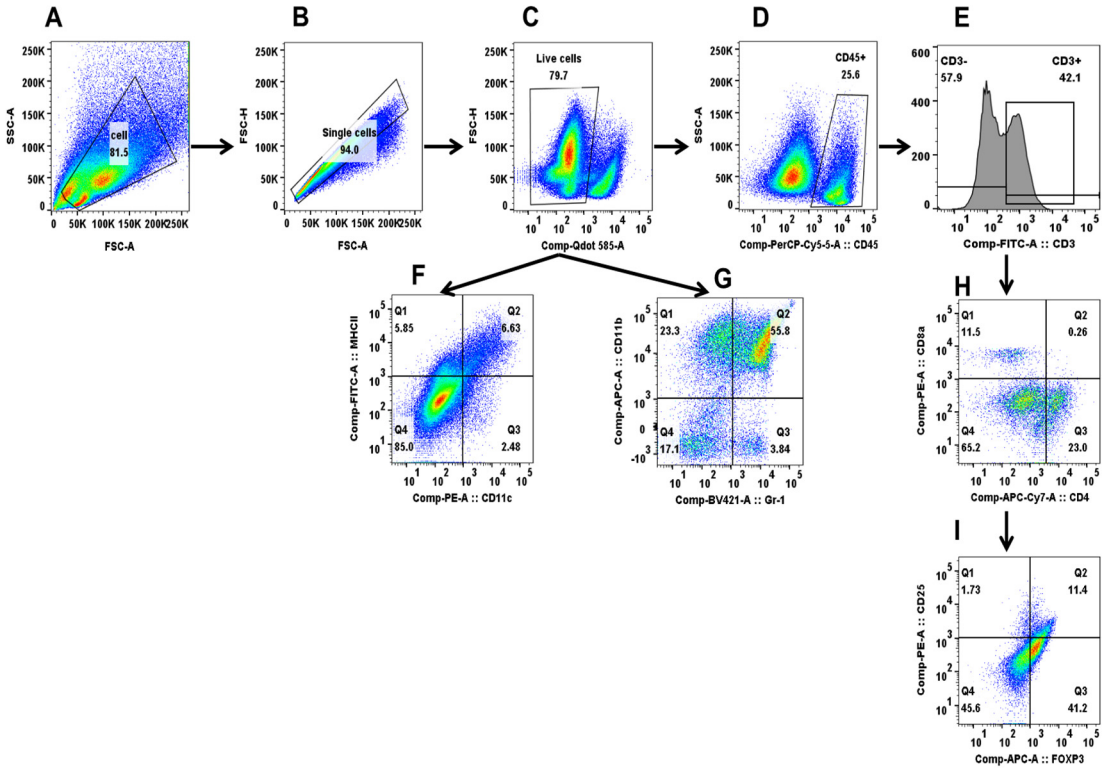

Figure S13. Gating strategy used for *in vivo* flow cytometry experiments. (A) All events were plotted side scatter vs. forward scatter, and debris was gated out. Next (B) single cells and (C) live cells were selected. To find DCs, CD11c+ and MHC-II+ cells were selected (F). To find MDSCs, CD11b+ and Gr-1+ cells were selected (G). Then, CD45+cells were selected for immune cell panels (D), CD3+ cells were selected for T cells (E). For adaptive immune cell studies, CD45+ and CD3+cells were selected for CD4 or CD8 positivity (H). Next, Tregs were quantified from CD45+ and CD4+cells that were also CD25+and FoxP3+ (I).

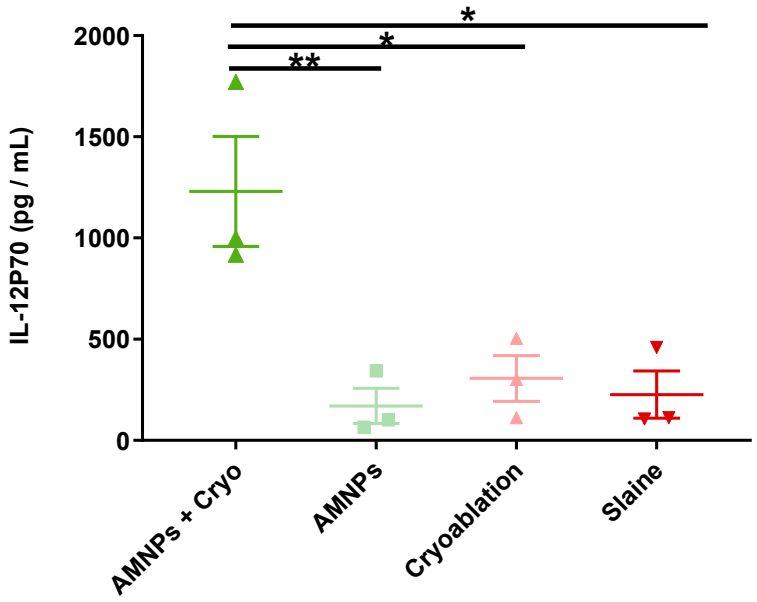

Figure S14. On Day 34, the concentration of IL-12 in the peripheral blood of mice was detected by the ELISA method.

Supplementary Table 1. P value of the heatmap differences between Saline group and Cryo+AMNPs group in Figure S11 (G).

	P value (four groups)	P value (Saline vs. Cryo+AMNPs group)
ADIPOGENESIS	0.028	0.044
APICAL_JUNCTION	0.028	0.014
APICAL_SURFACE	0.013	0.02
ESTROGEN_RESPONSE_EARLY	0.004	-
ESTROGEN_RESPONSE_LATE	0.001	0.005
FATTY_ACID_METABOLISM	0.026	-
HEME_METABOLISM	0.002	0.02
KRAS_SIGNALING_DN	0.004	0.002
MYOGENESIS	0	0
OXIDATIVE_PHOSPHORYLATION	0.015	0.004
PI3K_AKT_MTOR_SIGNALING	0.028	0.019

REACTIVE_OXYGEN_SPECIES_PATHWAY	0.047	0.038
UV_RESPONSE_UP	0.007	0.01
ANGIOGENESIS	-	0.047

“-” means P＞0.05

Figure S15. Curves of GSEA enrichment scores for the hallmark gene sets in Saline vs. Cryo+AMNPs group.

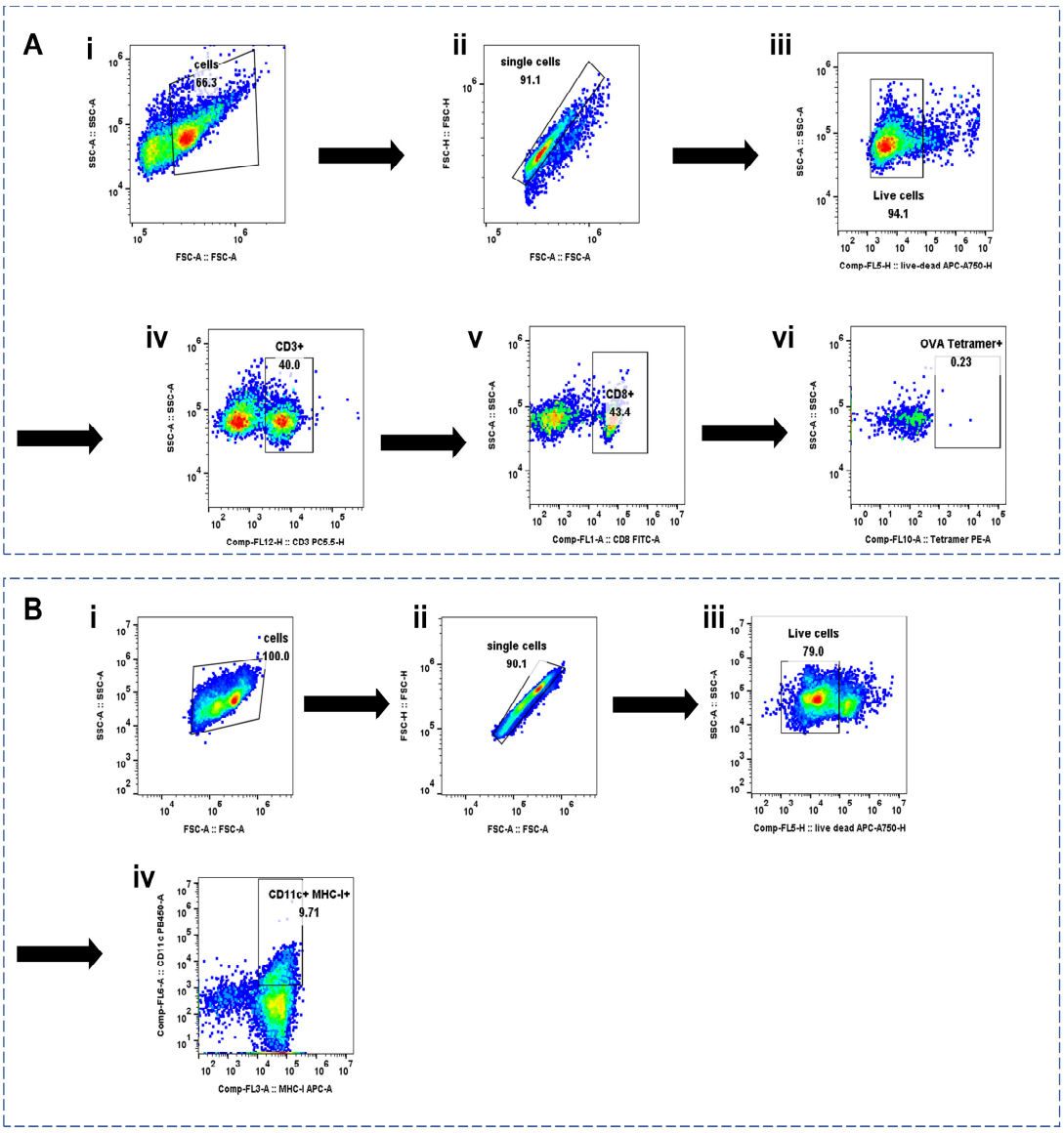

Figure S16. Gating strategy used for flow cytometry experiments. (A) OVA-specific T cells: (i)All events were plotted side scatter vs. forward scatter, and debris was gated out. Next (ii) single cells and (iii) live cells were selected. (iv)CD3+ cells were selected for T cells. (v) CD8+ cells were selected. (vi) OVA Tetramer+ cells were selected. (B) MHC-I dendritic cells: (i)All events were plotted side scatter vs. forward scatter, and debris was gated out. Next (ii) single cells and (iii) live cells were selected.(iv)To find DCs, CD11c+ and MHC-I+ cells were selected.

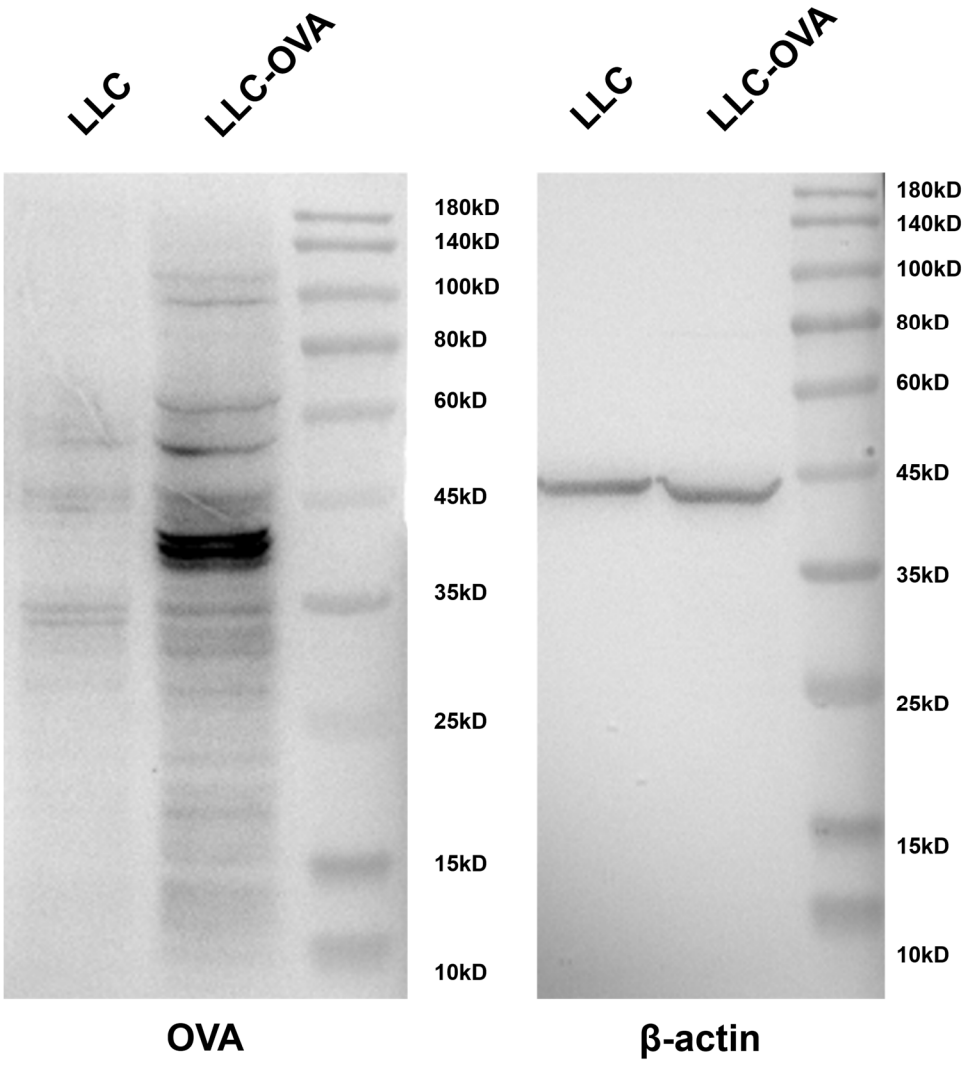

Figure S17. Western blot probing for OVA on LLC-OVA cells and control cells.